Cell, Vol. 92, 573–585, February 20, 1998, Copyright ©1998 by Cell Press

Orexins and Orexin Receptors: A Family of Hypothalamic Neuropeptides and G Protein-Coupled Receptors that Regulate Feeding Behavior

Takeshi Sakurai,[1,8] Akira Amemiya,[1,9] Makoto Ishii,[1] Ichiyo Matsuzaki,[1,10] Richard M. Chemelli,[1,2] Hirokazu Tanaka,[1] S. Clay Williams,[1] James A. Richardson,[3] Gerald P. Kozlowski,[4] Shelagh Wilson,[5] Jonathan R. S. Arch,[5] Robin E. Buckingham,[5] Andrea C. Haynes,[5] Steven A. Carr,[6] Roland S. Annan,[6] Dean E. McNulty,[6] Wu-Schyong Liu,[6] Jonathan A. Terrett,[5] Nabil A. Elshourbagy,[6] Derk J. Bergsma,[6] and Masashi Yanagisawa[1,7]

[1]Howard Hughes Medical Institute
Department of Molecular Genetics
[2]Department of Pediatrics
[3]Department of Pathology
[4]Department of Physiology
University of Texas Southwestern
Medical Center at Dallas
Dallas, Texas 75235–9050
[5]SmithKline Beecham Pharmaceuticals
Harlow, Essex CM19 5AD
United Kingdom
[6]SmithKline Beecham Pharmaceuticals
King of Prussia, Pennsylvania 19406

Summary

The hypothalamus plays a central role in the integrated control of feeding and energy homeostasis. We have identified two novel neuropeptides, both derived from the same precursor by proteolytic processing, that bind and activate two closely related (previously) orphan G protein-coupled receptors. These peptides, termed orexin-A and -B, have no significant structural similarities to known families of regulatory peptides. *prepro-orexin* mRNA and immunoreactive orexin-A are localized in neurons within and around the lateral and posterior hypothalamus in the adult rat brain. When administered centrally to rats, these peptides stimulate food consumption. *prepro-orexin* mRNA level is up-regulated upon fasting, suggesting a physiological role for the peptides as mediators in the central feedback mechanism that regulates feeding behavior.

Introduction

Members of the family of seven-transmembrane, G protein-coupled cell surface receptors (GPCRs) respond to a wide variety of signals, including photons, amines, lipids, peptides, and proteases. Ligand binding initiates intracellular signal transduction through the activation of heterotrimeric G proteins. All of the known small regulatory peptides (small peptide hormones and neuropeptides) exert their biological actions by acting on GPCRs. Recent efforts in genomics research have identified a large number of cDNA sequences that encode "orphan" GPCRs, i.e., putative GPCRs without known cognate ligands. Many of these orphan GPCRs are likely to be receptors for heretofore unidentified signaling molecules, including new peptide hormones and neuropeptides. GPCRs already represent the largest class of target molecules for drugs available in the clinic (Hardman et al., 1996). The orphan GPCRs therefore represent a fruitful resource for drug discovery (Stadel et al., 1997).

To approach these possibilities, we undertook a systematic biochemical search for endogenous peptide ligands for multiple orphan GPCRs, using a cell-based reporter system. These screening experiments led to the identification of a novel family of neuropeptides that bind to two closely related orphan GPCRs. We call these peptide ligands "orexins," after the Greek word orexis, which means appetite. The mRNA for the precursor of these peptides is abundantly and specifically expressed in the lateral hypothalamus and adjacent areas, a region classically implicated in the central regulation of feeding behavior and energy homeostasis (Oomura, 1980; Bernardis and Bellinger, 1993, 1996). These peptides stimulate food consumption when administered centrally, and their production is influenced by nutritional state of the animal. Here we report the identification and initial biological characterization of two orexins as well as their two receptors.

Results and Discussion

Purification and Structure of Orexins

Our general strategy was to screen high-resolution HPLC fractions of various tissue extracts for GPCR-agonist activity, using multiple orphan GPCR–expressing cell lines tested in parallel. For this purpose, we generated over 50 stable transfectant cell lines, each expressing a distinct orphan GPCR cDNA, which can be used as reporter cell lines in order to identify endogenous ligands for these receptors. We challenged the cells with HPLC fractions derived from tissue extracts and we monitored a number of signal transduction read-outs for heterotrimeric G protein activation. A potential problem in this approach is the presence of numerous endogenous GPCRs in the host cell line. To circumvent this problem in part, we assayed active fractions against at least 2–3 independent transfectant cell lines each expressing a different orphan GPCR. This enabled us to search for active fractions that activate only cells that express a specific receptor.

In this process, we discovered several reverse-phase HPLC fractions of rat brain extracts (Figure 1) that elicit a robust increase of cytoplasmic Ca^{2+} levels ($[Ca^{2+}]_i$) in HEK293 cells expressing an orphan GPCR originally

[7]To whom correspondence should be addressed.
[8]Present address: Institute of Basic Medical Sciences, University of Tsukuba, Ibaraki 3050006, Japan.
[9]Present address: First Department of Surgery, Osaka University Medical School, Osaka 5650871, Japan.
[10]Present address: Institute of Community Medicine, University of Tsukuba, Ibaraki 3050006, Japan.

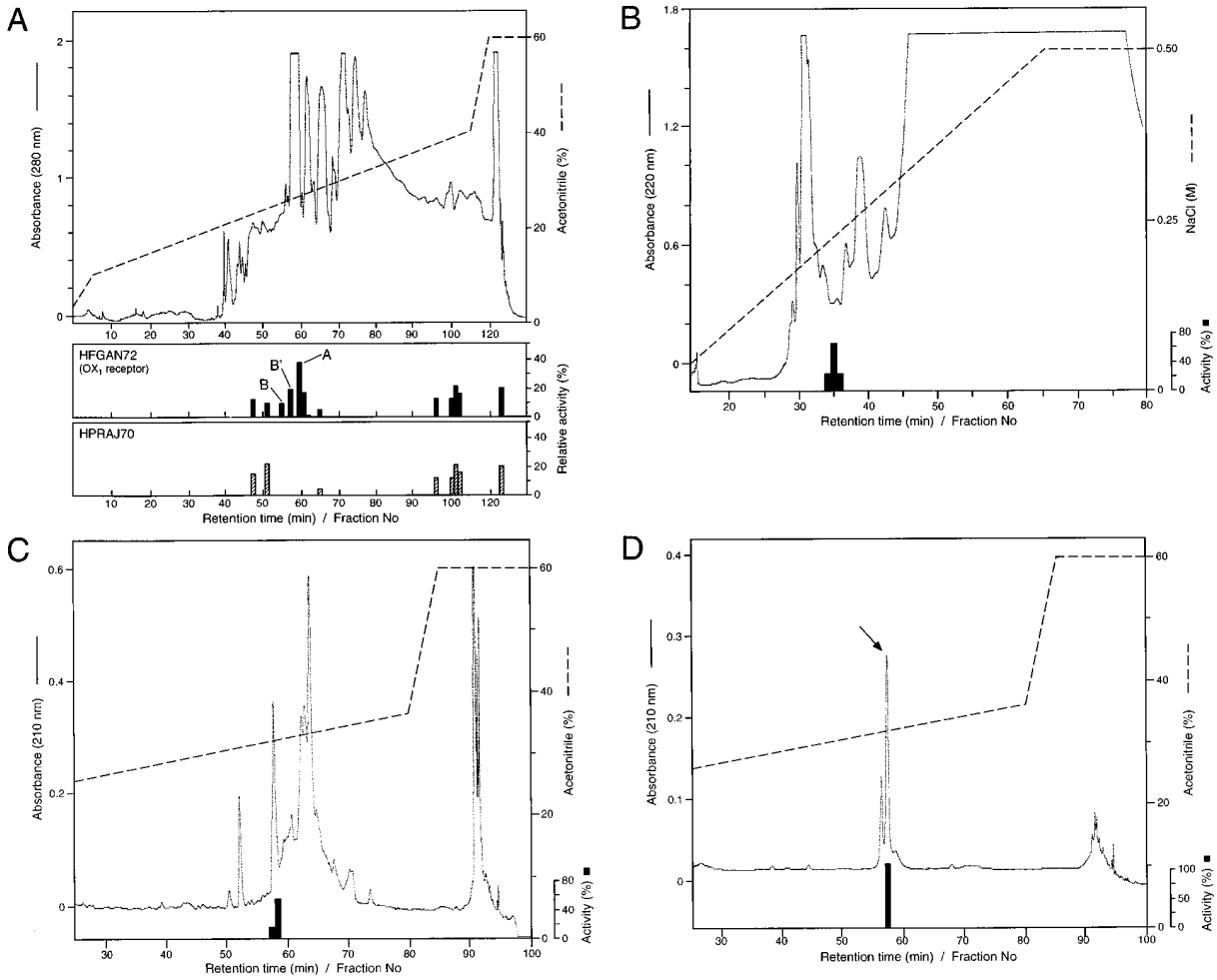

Figure 1. Purification of Endogenous Ligands for the Orphan Receptor HFGAN72 (OX_1R)

(A) Activation of the HFGAN72 receptor in transfected HEK293 cells by reverse-phase HPLC fractions of crude peptide extracts from rat brain. Top panel, chromatogram. Acetonitrile gradient and absorbance of eluted materials are indicated by solid and dotted lines, respectively. Middle and bottom panels, $[Ca^{2+}]_i$ transients in two HEK293 cell lines stably expressing unrelated orphan receptors *HFGAN72* and *HPRAJ70*, respectively. Peak increments in $[Ca^{2+}]_i$ evoked by designated HPLC fractions are normalized against the response induced by 100 nM endothelin-1 in the same reporter cell preparations and plotted as relative activity. Note that a number of fractions induced similar responses in both cell lines, presumably by acting on endogenous receptors in the host HEK293 cells. However, fractions 60–61 (marked as A; containing orexin-A) induced robust $[Ca^{2+}]_i$ transients in *HFGAN72*-transfected cells but not in *HPRAJ70*-transfected cells. Fractions 56 and 58 also exhibited weaker but distinct activities specific to HFGAN72 (marked as B and B′; containing orexin-B and orexin-B[3–28], respectively).

(B) Cation exchange HPLC of fractions 60–61 from Figure 1A. Bars show normalized magnitude of $[Ca^{2+}]_i$ in *HFGAN72*–expressing HEK293 cells as in Figure 1A.

(C) Reverse-phase HPLC of active fractions from Figure 1B.

(D) Final purification by reverse-phase HPLC at 40°C of active fractions in Figure 1C. Arrow, final orexin-A peak.

termed HFGAN72. This receptor was initially identified as an expressed sequence tag (EST) from human brain (see Figure 2C). A major activity peak (marked "A" in Figure 1A) was reproducibly accompanied by two additional minor peaks of activity (B and B′ in Figure 1A). These activities appeared to be specific for the HFGAN72 receptor, since the active fractions failed to evoke detectable $[Ca^{2+}]_i$ transients in cells expressing an unrelated orphan receptor, HPRAJ70, in a parallel assay (Figure 1A). These activities seemed to be peptidic, since protease treatment of the active fractions destroyed the activity.

We purified the major activity to homogeneity from acid-acetone extracts of rat brains by collecting active fractions after four steps of HPLC (Figure 1). The final purified material, corresponding to the absorbance peak at the arrow in Figure 1D, was subjected to structural analyses by limited protease digestions followed by nanoelectrospray tandem mass spectrometry, Edman degradation, and MALDI mass spectrometry (see Experimental Procedures for details). The active substance, termed orexin-A, was found to be a 33–amino acid peptide of 3,562 Da, with an N-terminal pyroglutamyl residue and C-terminal amidation (Figure 2A). Molecular mass of the peptide as well as its sequencing analyses indicated that the four Cys residues of orexin-A formed two sets of

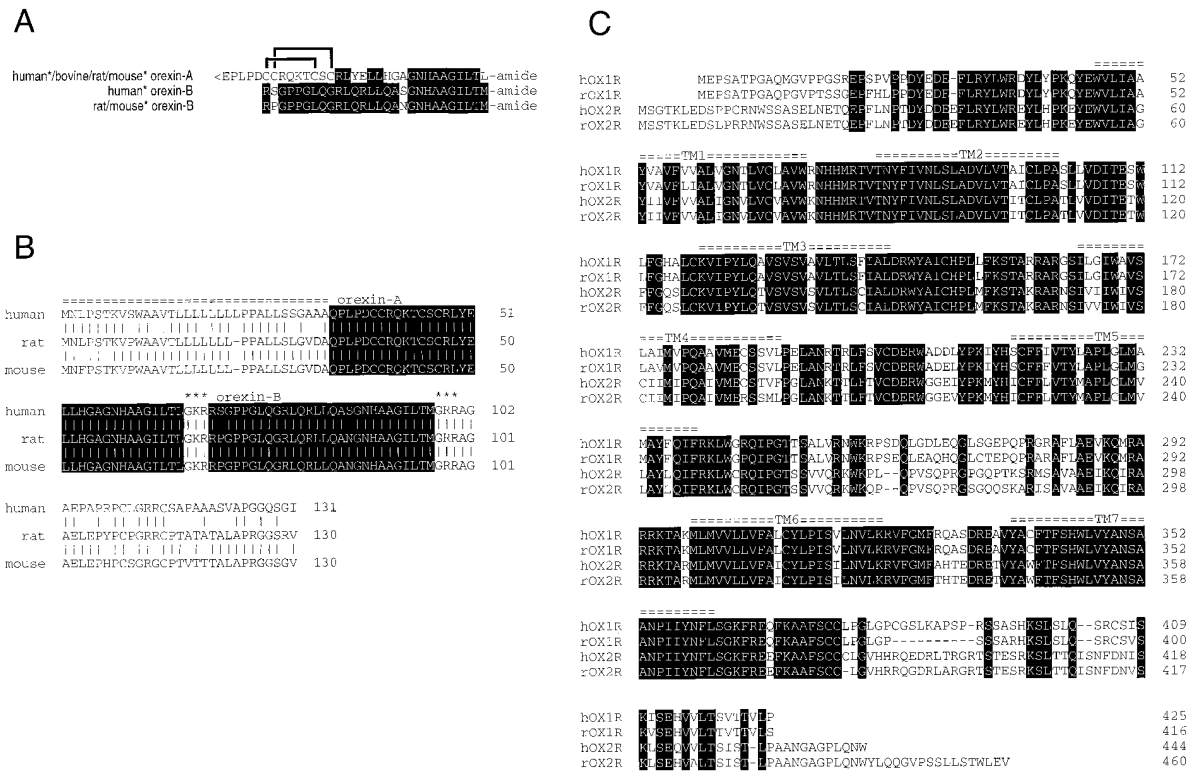

Figure 2. Amino Acid Sequences of Orexins and Orexin Receptors

(A) Structures of mature orexin-A and -B peptides. The topology of the two intrachain disulfide bonds in orexin-A is indicated above the sequence. The N-terminal pyroglutamyl residue (<E) in orexin-A is depicted. Amino acid identities are indicated by boxes. Asterisks indicate that human and mouse sequences are deduced from the respective genomic sequences and not from purified peptides.

(B) Deduced amino acid sequences of prepro-orexin precursor polypeptides. Orexin-A and -B sequences are boxed. Secretory signal sequences predicated by the SignalP Server (http://www.cbs.dtu.dk/services/SignalP/) are marked by equal signs (=); prohormone convertase cleavage and amidation sites by asterisks (*). Interspecifically identical residues are indicated by vertical bars. The full-length nucleotide sequences of human, rat, and mouse prepro-orexin cDNAs have been submitted to GenBank (accession numbers AF041240, AF041241, and AF041242).

(C) Deduced amino acid sequences of rat (r) and human (h) OX_1 and OX_2 receptors. Amino acid residues that are identical in all four sequences are boxed. Putative transmembrane (TM) domains are marked above the aligned sequences, as predicted by the PredictProtein server (http://www.embl-heidelberg.de/predictprotein). Gaps introduced to obtain optimal alignment are indicated by dashes. The full-length nucleotide sequences of human and rat orexin receptor cDNAs have been submitted to GenBank (accession numbers AF041243, AF041244, AF041245, and AF041246).

intrachain disulfide bonds. The topology of the disulfide bonds was determined by selectively synthesizing the peptides with different disulfide topologies by using selective deprotection and sequential oxidation of two of the four Cys residues and then comparing these synthetic peptides with purified natural orexin-A in isocratic reverse-phase HPLC. The topology was determined to be [Cys6-Cys12, Cys7-Cys14] (Figure 2A). Using similar protocols, we also purified the analogous activity from bovine hypothalamic extracts, and we found that the structure of bovine orexin-A was identical to that of the rat peptide.

In addition to the major peak of activity, the HPLC fractions contained two minor activity peaks that we designated B and B′ (Figure 1A). We isolated peptides responsible for both of these activities from rat brain extracts using similar purification protocols (see Experimental Procedures). Mass spectrometry and Edman sequencing showed that peak B contained a 28–amino acid, C-terminally amidated linear peptide of 2,937 Da. The peptide, termed orexin-B, was 46% (13/28) identical in sequence to orexin-A (Figure 2A). Peak B′ contained an N-terminally truncated [des Arg-Pro]orexin-B, which we designate orexin-B[3–28]. Further investigation is required to determine whether this truncation represents a physiologically relevant processing or whether it is a result of an artifactual proteolysis during the extraction procedure. In the subsequent studies described below, only orexin-A and full-length orexin-B were subjected to further biological characterization.

Structure of the Prepro-Orexin Precursor

The amino acid sequences of purified orexin-A and -B exhibited no meaningful similarity to any known peptides. A BLAST search of the GenBank database also failed to detect an entry that contains these or similar sequences. Therefore, we sought to isolate the cDNA encoding the precursor polypeptide; we first obtained a cDNA fragment encoding a part of orexin-A by RT–PCR of rat brain mRNA, using highly degenerate primers

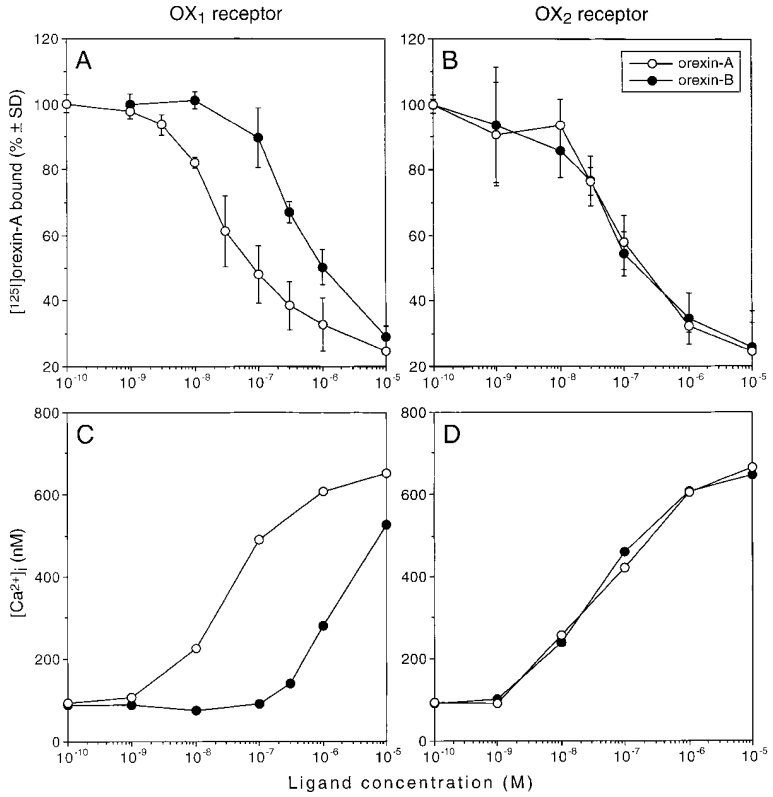

Figure 3. Pharmacological Characterization of Synthetic Human Orexins on Human Orexin Receptors Expressed in Stably Transfected CHO Cells

(A and B) Competitive radioligand binding assays. Displacement of [^{125}I-Tyr17]orexin-A binding to cells expressing human *OX$_1$R* (A) and *OX$_2$R* (B) by increasing concentrations of unlabeled orexin-A (open circle) and human orexin-B (filled circle) are determined in quadruplicates. Level of nonspecific binding was approximately 20% of the binding in the absence of competitor.

(C and D) Dose-response relationships of $[Ca^{2+}]_i$ transients evoked by orexin-A (open circle) and human orexin-B (filled circle) in cells expressing human *OX$_1$R* (C) and *OX$_2$R* (D). Peak $[Ca^{2+}]_i$ values are determined in duplicates.

based on parts of the orexin-A sequence. We then performed 5′-RACE and 3′-RACE reactions to obtain the full-length cDNA. We found that this cDNA encoded both orexin-A and -B (Figures 2A and 2B).

The 5′-most ATG codon of the 585 bp cDNA (GenBank accession number AF041241) was preceded by an in-frame stop codon, and the sequence around this initiation codon conformed to Kozak's rules. The open reading frame starting with this ATG encodes a 130-residue polypeptide, the rat prepro-orexin (Figure 2B). The first 33 amino acids exhibited characteristics of a secretory signal sequence: a hydrophobic core followed by residues with small polar side chains (von Heijne, 1986). The SignalP Server web site predicted that Ala32-Gln33 was the most likely site for signal sequence cleavage. The orexin-A sequence starts with Gln33, which is presumably cyclized enzymatically into the N-terminal pyroglutamyl residue by transamidation (Busby et al., 1987; Bateman et al., 1990). Thus, the mature peptide directly follows the signal peptide cleavage site. The last residue of the mature peptide is followed by Gly66, which presumably serves as NH_2 donor for C-terminal amidation by sequential actions of peptidylglycine monooxygenase and peptidylamidoglycolate lyase (Bradbury and Smyth, 1991; Eipper et al., 1993). As expected, Gly66 is followed by a pair of basic amino acid residues, Lys67-Arg68, which constitute a recognition site for prohormone convertases (Rouille et al., 1995). The next segment of the deduced prepro-orexin sequence, Arg69-Met96, was identical to the sequence of purified orexin-B. The Met96 residue is again followed by Gly-Arg-Arg, a C-terminal amidation signal, consistent with our finding that orexin-B is also C-terminally amidated.

We isolated human and mouse genomic fragments containing the *prepro-orexin* gene in order to predict the sequences of the human and mouse prepro-orexin polypeptides. Details of the gene structure will be reported elsewhere. The predicted human and mouse orexin-A sequences were both identical to rat and bovine orexin-A (Figure 2A). Mouse orexin-B was also predicted to be identical to rat orexin-B. Human orexin-B had two amino acid substitutions when compared with the rodent sequence (Figure 2A). Overall, the human and mouse prepro-orexin sequences were 83% and 95% identical to their rat counterparts, respectively. A majority of amino acid substitutions were found in the C-terminal part of the precursor, which appears unlikely to encode for another bioactive peptide.

Radiation hybrid mapping showed that the human *prepro-orexin* gene is most tightly linked to the MIT STS markers WI-6595 and UTR9641. The inferred cytogenetic location between these markers is 17q21. Interestingly, the localization at chromosome 17q21 raises the possibility that the prepro-orexin gene may be a candidate gene for a group of neurodegenerative disorders collectively called "chromosome 17-linked dementia" (Wilhelmsen, 1997), including nosological entities such as disinhibition-dementia-parkinsonism-amyotrophy complex (*DDPAC*; MIM No. *600274) and pallido-pontonigral degeneration (*PPND*; MIM No. *168610), which

may be caused by allelic mutations. Both *DDPAC* and *PPND* have recently been mapped to 17q21–22 (Wilhelmsen et al., 1994; Wijker et al., 1996).

Characterization of Orexin Receptors

Figure 2C shows the deduced amino acid sequences of the original HFGAN72 receptor, which we now call OX_1 receptor (OX_1R). Among various classes of GPCR, OX_1R is structurally most similar to certain neuropeptide receptors, most notably to the Y2 neuropeptide Y (NPY) receptor (26% identity), followed by the TRH receptor, cholesystokinin type-A receptor, and NK2 neurokinin receptor (25%, 23%, and 20% identity, respectively). This is consistent with our hypothesis that OX_1R is the receptor for orexins, another class of small regulatory peptides. In order to characterize further their pharmacological interactions, we performed in vitro functional assays using transfected cell lines expressing the receptor. Mock transfected CHO cells did not exhibit detectable levels of specific binding of radio-iodinated [^{125}I-Tyr17]orexin-A. Stable transfection of CHO cells with an expression vector containing the human *OX_1R* cDNA (CHO/OX_1R) conferred the ability to bind [^{125}I]orexin-A (Figure 3A). The radioligand binding was inhibited by nanomolar concentrations of unlabeled synthetic orexin-A in a dose-dependent manner, but not by any of several unrelated peptides tested, including human NPY and endothelin-1 at up to 10 μM (data not shown). The concentration of unlabeled orexin-A required to displace 50% of specific radioligand binding (IC_{50}) was 20 nM as calculated by the LIGAND program (Munson and Rodbard, 1980). Orexin-A also induced a transient increase in $[Ca^{2+}]_i$ in CHO/OX_1R cells in a dose-dependent manner (Figure 3C), but failed to induce detectable $[Ca^{2+}]_i$ transients in mock transfected CHO cells. We feel that the calcium mobilization is likely caused by the activation of the Gq class of heterotrimeric G proteins (Hepler et al., 1994). The calculated concentration of orexin-A required to induce half-maximum response (EC_{50}) was 30 nM. We obtained similar results in radioligand binding and $[Ca^{2+}]_i$ transient assays performed with stably transfected HEK293 cells (data not shown). These findings confirm that orexin-A is indeed a specific, high-affinity agonist for OX_1R.

As expected from our purification experiments, synthetic human orexin-B also acted as a specific agonist on CHO/OX_1R cells in a parallel set of experiments (Figures 3A and 3C). Interestingly, however, we found that human orexin-B has significantly lower affinity for the human OX_1R: the calculated IC_{50} in the competitive binding assay and the EC_{50} in the $[Ca^{2+}]_i$ transient assay were 420 nM and 2500 nM for human orexin-B, respectively, indicating 2–3 orders of magnitude lower affinities as compared with orexin-A. Similar results were obtained with HEK293 cells expressing *OX_1R*.

The findings with orexin-B led us to suspect that there is an additional orexin receptor(s) for which orexin-B has high affinity. A BLAST (tblastn) search of the GenBank dbEST database with the OX_1R amino acid sequence detected two highly similar EST entries: accession numbers D81887 (human fetal brain cDNA) and W86548 (human fetal liver/spleen cDNA). These EST sequences

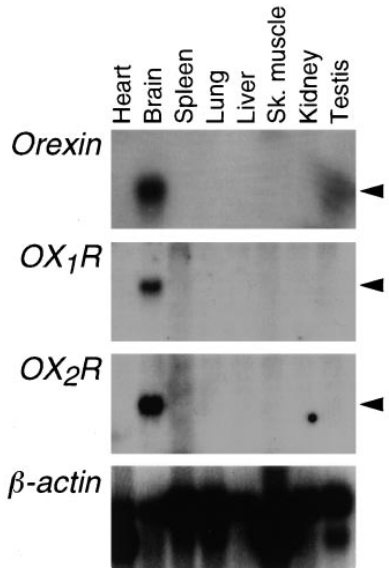

Figure 4. Tissue Distribution of Rat *prepro-orexin* and Orexin Receptor mRNAs

A membrane containing ~2 μg/lane of poly(A)$^+$ RNA from indicated rat tissues (Clontech, cat. no. 7764–1) was sequentially rehybridized with designated cDNA probes using standard methods. Sizes of *prepro-orexin*, *OX_1R* and *OX_2R* mRNAs are approximately 0.7, 2.5, and 3.5 kb, respectively (arrowheads). A segment of rat *prepro-orexin* cDNA encoding Gln33-Ser128 (Figure 2B) as well as full-length rat *OX_1R* and *OX_2R* cDNAs (Figure 2C) were used as probes. These probes do not detectably cross-hybridize with each other under the high-stringency conditions used. Autoradiography was exposed for 5 days, 3 days, 3 days and 3 hr for *prepro-orexin*, *OX_1R*, *OX_2R*, and β-*actin* probes.

showed much higher similarities to the OX_1R sequence than to numerous other GPCR entries. At the nucleotide sequence level, they differed enough from the human *OX_1R* cDNA sequence to indicate that they are not derived from the *OX_1R* gene itself. We subsequently found that these two ESTs were derived from 5′ and 3′ parts of the same transcript. Full-length cloning and sequencing showed that this cDNA encodes a GPCR, termed OX_2R, that highly resembles OX_1R (Figure 2C). The amino acid identity between the deduced full-length human OX_1R and OX_2R sequences is 64%. Thus, these receptors are much more similar to each other than they are to other GPCRs. Amino acid identities between the human and rat homologs of each of these receptors are 94% for OX_1R and 95% for OX_2R, indicating that both receptor genes are highly conserved between the species.

To characterize functionally the OX_2R further, we repeated competitive radioligand binding assays and $[Ca^{2+}]_i$ transient dose-response studies using stably transfected CHO cells expressing the human *OX_2R* cDNA. The results demonstrated that OX_2R is indeed a high-affinity receptor for human orexin-B, with an IC_{50} of 36 nM in the binding assay and an EC_{50} of 60 nM in the $[Ca^{2+}]_i$ transient assay (Figures 3B and 3D). Orexin-A also had high affinity for this receptor, with 38 nM IC_{50} and 34 nM EC_{50} values, which are similar to the values for orexin-B. Thus, we conclude that OX_2R is a nonselective

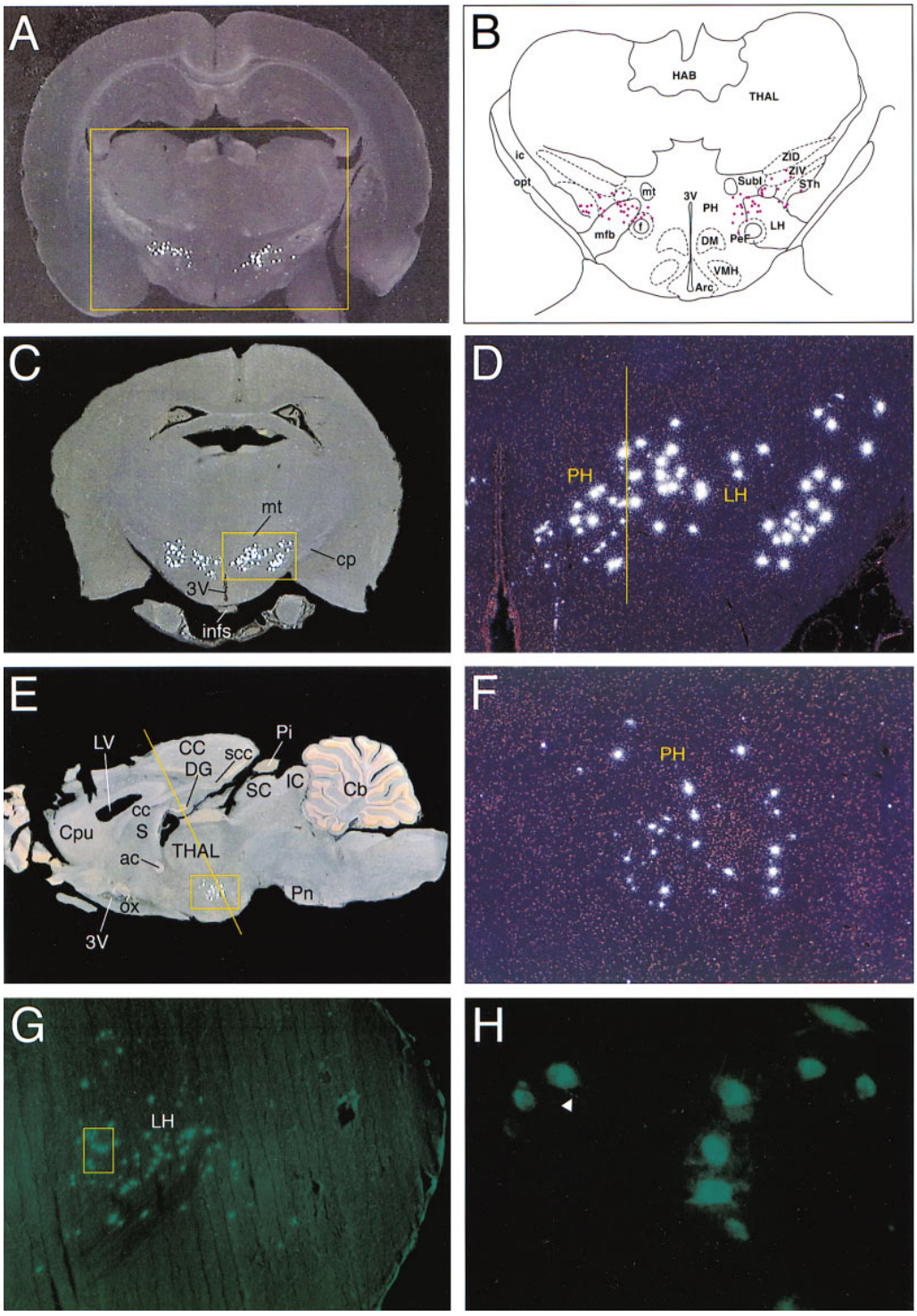

Figure 5. Localization of *prepro-orexin* mRNA and Immunoreactive Peptide in Adult Rat Brain

(A) Visualization of neurons containing *prepro-orexin* mRNA in the adult rat hypo- and subthalamic areas by in situ hybridization. Coronal section of brain hybridized with ^{35}S-labeled anti-sense riboprobe showing the bilateral and symmetrical distribution of labeled neurons. No detectable signal beyond background was generated by sense riboprobe. The yellow rectangle designates the area schematized in Figure 5B.

(B) *prepro-orexin* mRNA–containing neurons are shown in red superimposed upon anatomical structures of the hypo- and subthalamic areas (Paxinos and Watson, 1986): lateral hypothalamic area (LH), perifornical nucleus (PeF), posterior hypothalamic area (PH), subthalamic nucleus (Sth), subincertal nucleus (SubI), and ventral zona incerta (ZIV). Additional landmarks include: thalamus (THAL), habenular complex (HAB), internal capsule (ic), optic tract (opt), mammillothalamic tract (mt), fornix (f), medial forebrain bundle (mfb), third ventricle (3V), arcuate hypothalamic nucleus (Arc), dorsomedial hypothalamic nucleus (DM), and ventromedial hypothalamic nucleus (VMH). (Permission for use granted by Academic Press.)

receptor for both orexin-A and -B, while OX_1R is selective for orexin-A.

In radiation hybrid mapping, the MIT markers showing tightest linkage to the human *OX_1R* and *OX_2R* genes are the STS markers D1S195 and D1S443, and WI-5448 and CHLC.GATA74F07, respectively. The inferred cytogenetic locations between these markers are 1p33 for *OX_1R*, and 6cen (p11-q11) for *OX_2R* (accurate cytogenetic locations are often difficult to interpret from radiation hybrid maps in which the gene lies near the centromere).

Tissue Distribution of Orexin and Orexin Receptors

N-terminal pyroglutamyl cyclization (seen in orexin-A) as well as C-terminal amidation (both orexin-A and -B) are posttranslational modifications that are most often found in neuropeptides. Northern blot analysis of adult rat tissues showed that the 0.7 kb *prepro-orexin* mRNA is detected exclusively in the brain except, in a small amount, in the testis (Figure 4). In adult rats, *OX_1R* and *OX_2R* mRNAs were also detected exclusively in the brain (Figure 4). These findings are consistent with the idea that orexins are regulatory peptides that function within the central nervous system.

Preliminary Northern blot analysis of human mRNA from multiple brain regions (human brain blots II and III, Clontech) demonstrated that the *prepro-orexin* mRNA was expressed abundantly in subthalamic nucleus, but undetectable in other brain regions tested (data not shown; hypothalamus was not included in these brain blots). *prepro-orexin* mRNA was also undetectable in the human heart, placenta, lung, liver, skeletal muscle, kidney, and pancreas (data not shown). These findings are consistent with the results of the in situ hybridization in the rat brain described below.

Distribution of Orexin–Containing Neurons in Rat Brain

To further localize orexin expression within the central nervous system, we performed in situ hybridization and immunohistochemical analyses in rat brains. In situ hybridization with a rat *prepro-orexin* cRNA probe in coronal sections showed orexin–containing neurons organized bilaterally and symmetrically in a discrete set in hypothalamic and subthalamic areas of the adult rat brain (Figures 5A–5D). In the hypothalamus, positive neurons were found in the lateral (Figures 5A–5H) and posterior hypothalamic areas (Figures 5A–5F) and the perifornical nucleus (Figures 5C–5F). In the subthalamus (also called ventral thalamus), the zona incerta, subincertal, and subthalamic nuclei were positive (Figure 5B). Both in situ hybridization histochemistry (Figures 5A and 5C–5F) and immunofluorescent cytochemistry labeled the cytoplasm of medium-sized neurons (Figures 5D–5H), showing identical distributions. The shapes of the neurons varied from thin and fusiform to robust and multipolar. It is noteworthy that no signal was detected in neurons of the paraventricular (not shown), ventromedial (Figure 5B), or arcuate nuclei (Figure 5B), which are known to contain a variety of neuropeptides associated with food consumption (Bernardis and Bellinger, 1996; Bing et al., 1996; see below).

Stimulation of Feeding Behavior by Centrally Administered Orexins

The lateral hypothalamic area has been implicated in the regulation of feeding behavior and energy homeostasis ever since the classic experiments showing that animals with lateral hypothalamic lesions had decreased food intake and lower "set point" for body weight (Oomura, 1980; Bernardis and Bellinger, 1993, 1996). The striking localization of orexin–containing neurons in the lateral hypothalamus and some of its adjacent areas suggested to us the possibility that the neuropeptide may be involved in the regulation of food intake. To evaluate this hypothesis, we administered orexin acutely into the lateral ventricle of male rats through preimplanted indwelling catheters. When a bolus was administered intracerebroventricularly in early light phase, orexin-A stimulated food consumption in a dose-dependent manner within 1 hr (Figure 6, left). The magnitudes of stimulation with 3 nmol and 30 nmol orexin-A the 2 hr time point were 6- and 10-fold, respectively. The effect persisted at 4 h; the amount of food consumed during the interval from 2–4 h postinjection was increased approximately 3-fold with either dose as compared to vehicle controls. Human orexin-B also significantly augmented food intake; at the 2 hr time point, we observed 5- and 12-fold stimulation of food consumption by 3 nmol and 30 nmol orexin-B, respectively, as compared with vehicle controls (Figure

(C) Low magnification of section caudal to Figure 5A showing the distribution of *prepro-orexin* mRNA–containing neurons. Mammillothalamic tract (mt), third ventricle (3V), cerebral peduncle (cp), infundibular stem (Infs). There are two groups of neurons: one group is seen in the posterior hypothalamus (PH) and the other in the lateral hypothalamus (LH). The yellow rectagle indicates the field shown in Figure 5D.

(D) Higher magnification of the neuronal cell bodies in Figure 5C. The yellow vertical line indicates the boundary separating the medial neurons of PH and the neurons of LH.

(E) Low magnification of *prepro-orexin* mRNA–containing neurons seen in parasagittal section traversing the posterior hypothalamic area shown in Figure 5D. Cerebral cortex (CC), dentate gyrus (DG), splenium of the corpus callosum (scc), lateral ventricle (LV), caudate putamen (Cpu), corpus callosum (cc), septum (S), anterior commissure (ac), thalamus (THAL), optic chiasm (ox), third ventricle (3V), pineal gland (Pi), superior colliculus (SC), inferior colliculus (IC), cerebellum (Cb), and pontine nucleus (Pn). The yellow rectagle indicates the field magnified in Figure 5F.

(F) High-magnification of the *prepro-orexin*–expressing neurons in the posterior hypothalamus (PH) shown in Figure 5E.

(G) Orexin-A-immunoreactive neurons in the LH of a frozen parasagittal section. Dorsal aspect is to the left side of this panel. The yellow box corresponds to the field shown in Figure 5H. The staining of orexin-A-positive neurons was abolished in the presence of excess (100 nM) synthetic orexin-A.

(H) High magnification of the immunoreactive orexin–containing neurons of the LH area. The boxed area of cells Figure 5G have been rotated 90° clockwise. In general, most of the neurons are multipolar, but a few are fusiform. The nucleus is not immunopositive, indicating that orexin is cytoplasmic. Beaded neuronal processes are sometimes seen in these sections (arrowhead).

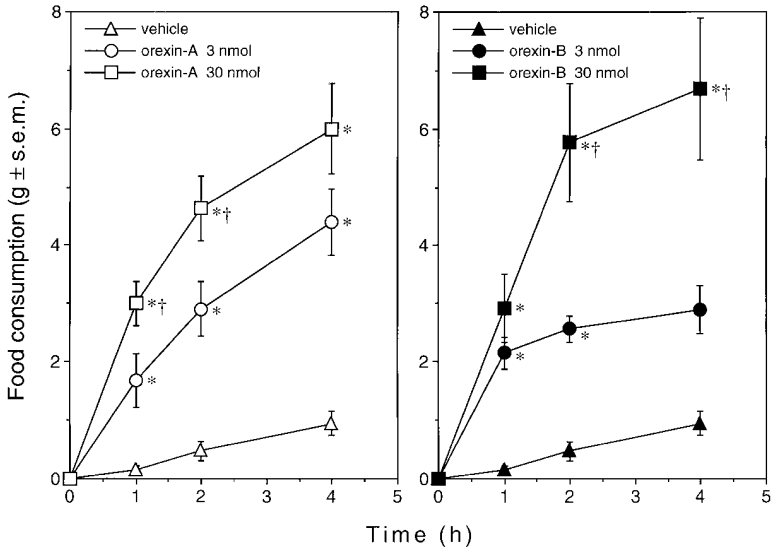

Figure 6. Stimulation of Food Consumption by Intracerebroventricular Injection of Orexin-A and -B in Freely Fed Rats

Designated amounts of synthetic human orexin-A (left) or -B (right) were administered in a 5 μl bolus through a catheter placed in the left lateral ventricle in early light phase. Cumulative food consumption was plotted over the period of 4 hr after injection. Asterisks (*) indicate significant difference from vehicle controls ($p < 0.05$, $n = 8–10$, ANOVA followed by Student-Newman-Keuls test). Crosses (†) designate significant difference between 3 nmol and 30 nmol injections ($p < 0.05$, $n = 8–10$, ANOVA followed by Student-Newman-Keuls test). Similar results were obtained in at least four independent sets of experiments. The same vehicle control curve was replotted in both panels.

6, right). The effects of orexin-B did not last as long as those of orexin-A; there was little stimulation of food intake after 2 hr even with the higher dose. These actions of orexin were less efficacious than NPY, a known orexigenic neuropeptide (Gerald et al., 1996; Turton et al., 1996), but longer lasting in the case of orexin-A; under the same conditions, we found that 3 nmol human NPY induced cumulative food consumption of 11.4 ± 2.0 g and 12.8 ± 1.8 g (mean ± SEM) at 2 hr and 4 hr internals, respectively, representing 24- and 14-fold stimulation over vehicle controls.

The shorter action of orexin-B as compared with orexin-A might be related to the fact that orexin-B is a linear peptide with a free N terminus. In contrast, both termini of orexin-A are blocked by posttranslational modifications. Together with the two intrachain disulfide bonds, these modifications may render orexin-A resistant to inactivating peptidases. We cannot exclude the possibility that these time courses reflect bona fide differences in the biological actions of orexin-A and orexin-B in the central nervous system. The similar degrees of stimulation of food intake by both orexin-A and orexin-B suggest that OX_2R, the nonselective receptor (see Figure 3), may at least in part be involved in this in vivo pharmacological action of orexins. However, more detailed in vivo dose-response studies, as well as a separate blockade of these receptors either pharmacologically by selective antagonists or genetically by gene targeting, will be required to determine the receptor(s) involved.

Up-Regulation of *prepro-orexin* mRNA in the Fasting State

The stimulation of food intake by centrally administered orexins suggested that these neuropeptides may play a physiological role in the central regulation of feeding. To evaluate the possibility that orexin production and release may be affected by nutritional state, we compared the level of *prepro-orexin* mRNA expression in the hypothalamus of fed and fasted rats. Adult male rats were housed singly under 12 hr light-dark cycle for at least 5 days, and then either fed ad libitum ($n = 5$) or fasted for 48 hr starting at mid-light cycle ($n = 5$). At the end of the 48 hr period, rats were sacrificed and the thalamic/hypothalamic portion of the brain was dissected. Total RNA was extracted from individual samples and subjected to quantitative Northern blot analysis. After the 48 hr fast, hypothalamic *prepro-orexin* mRNA was up-regulated 2.4-fold as compared with the fed control animals (Figure 7). *NPY* mRNA was previously described to be up-regulated under similar fasted conditions (Qu et al., 1996). We also found that *NPY* mRNA was up-regulated, albeit to a lesser extent than the orexin mRNA (Figure 7A).

Physiological Implications

Quantum leaps in our understanding of the mechanisms involved in the energy homeostasis have resulted from the recent identification of the leptin signaling pathway (Zhang et al., 1994; Chen et al., 1996) and by additional molecular genetic studies in mice. These studies have revealed a number of central regulatory pathways mediated by various neuropeptides (Yen et al., 1994; Erickson et al., 1996a; Huszar et al., 1997; Ohki-Hamazaki et al., 1997). Maintenance of body weight is achieved by an intricate balance between energy intake (food consumption) and expenditure. This energy homeostasis is ultimately governed by the brain, where a variety of afferent signals reflect the animal's nutritional state and its external environment, particularly food availability. These signals are integrated in order to moderate efferent pathways that control feeding behavior and energy expenditure (Bray, 1995; Rosenbaum et al., 1997). The afferent signals include somatic sensory signals like smell and taste, gastrointestinal signals like mechanical distention and chemical stimuli to the mucosa, blood-born metabolites like glucose and free fatty acids, and "lipostatic" signals such as leptin (Friedman, 1997). Together with the regulation of metabolic rate, which is in part mediated by sympathetic and parasympathetic nervous systems and thyroid hormone, the regulation of feeding behavior constitutes the efferent wing of energy homeostasis. The central site of integration is the hypothalamus (Oomura, 1980; Bernardis and Bellinger, 1993, 1996),

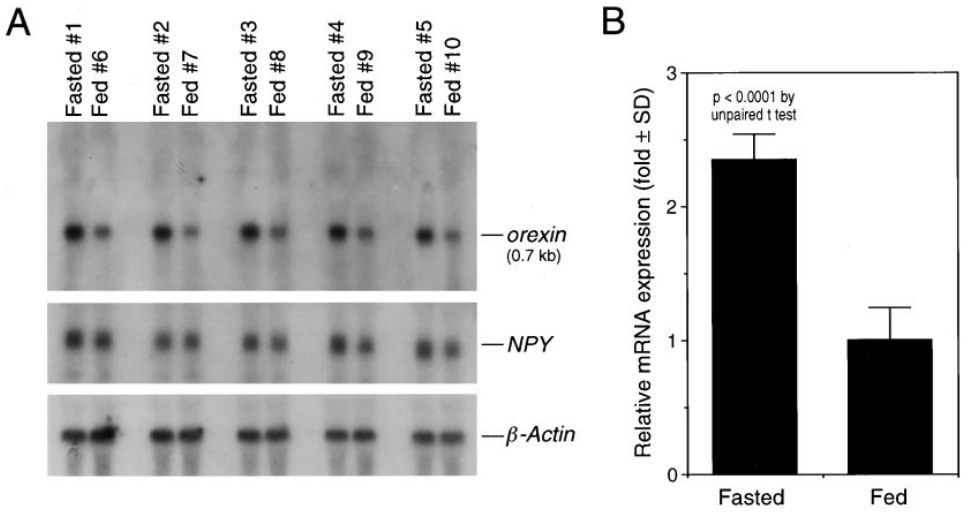

Figure 7. Up-Regulation of *prepro-orexin* mRNA in Fasted Rats

(A) Northern blot analysis of hypothalamic *prepro-orexin* mRNA expression in freely fed and 48 hr fasted rats. Each lane contains 20 μg of total RNA from rat diencephalon. The membrane was rehybridized with *NPY* cDNA and then with β-*actin* cDNA as internal reference for the amount of RNA loaded.

(B) Densitometric quantitation of Northern blot results presented in Figure 7A. The ratio of *prepro-orexin* and β-*actin* mRNA signals was determined in each lane, and these normalized values were then compared between the fasted and fed groups. The mean value for normalized *prepro-orexin* mRNA expression in the fed group was arbitrarily designated as unity.

where a large array of neurotransmitters, especially neuropeptides, modulate signals through complex neural circuits.

Recent molecular genetic studies in rodents have started to provide convincing evidence supporting important roles for certain hypothalamic neuropeptides in the central regulation of energy balance (Wolf, 1997). For example, NPY, which is negatively regulated by leptin (Zarjevski et al., 1993; Stephens et al., 1995; Tartaglia et al., 1995), has been established as one of the positive regulators of feeding behavior, presumably acting on the Y5 NPY receptor (Gerald et al., 1996); thus, the obesity of leptin-deficient mice is partially ameliorated when they are also deficient in NPY (Erickson et al., 1996b). Ectopic and constitutive expression of the endogenous antagonist for melanocortin receptors, the Agouti protein, is the basis of obesity in obese-yellow mice (Yen et al., 1994; Fan et al., 1997), and, indeed, deficiency in the MC4 melanocortin receptor completely replicates the obesity syndrome of obese-yellow mice (Huszar et al., 1997). Furthermore, Agouti-related protein (also termed ART), another endogenous antagonist for the MC4 receptor, has recently been shown to be expressed in the hypothalamus, and the expression is up-regulated in *ob/ob* and *db/db* mice (Ollmann et al., 1997; Shutter et al., 1997). More recently, mice deficient for an orphan neuropeptide receptor (bombesin receptor type-3) have also been shown to become obese (Ohki-Hamazaki et al., 1997). Within the hypothalamus, two regions have traditionally been associated with the regulation of feeding and energy balance: the ventromedial hypothalamus and the lateral hypothalamic area. A classical series of lesion experiments led to the hypothesis that the ventromedial hypothalamus functions as a "satiety center," whereas the lateral hypothalamic area works as a "feeding center." Thus, a lateral hypothalamic lesion causes the animal to eat less and lose weight, sometimes leading to death by starvation. While clearly oversimplified, these hypotheses still provide a valid conceptual framework (Oomura, 1980).

Recent studies continue to reveal the molecular basis for the role of periventricular/medial hypothalamic regions in energy homeostasis, e.g., ventromedial nucleus, arcuate nucleus, and paraventricular nucleus. Neurons containing neuropeptides such as NPY (Bing et al., 1996), melanocortins (Jacobowitz and O'Donohue, 1978), glucagon-like peptide-1 (Shughrue et al., 1996), and galanin (Warembourg and Jolivet, 1993), as well as the leptin and melanocortin-4 receptors (Mountjoy et al., 1994; Tartaglia et al., 1995) are abundant in one or more of these periventricular/medial hypothalamic regions. In contrast, few neuropeptides have been described to be produced chiefly in the lateral hypothalamic regions. Other than the orexins, we are aware of only one distinct neurotransmitter that is specifically produced in the lateral hypothalamus: melanin concentrating hormone (MCH) has been localized in the zona incerta and the lateral hypothalamic area (Bittencourt et al., 1992). Intriguingly, MCH was recently reported to stimulate food intake upon central administration. Moreover, *MCH* mRNA is up-regulated in *ob/ob* mice and by fasting in wild-type mice (Qu et al., 1996). It will be important to investigate further the possible interplay of orexin with this and other positive (e.g., Agouti-related protein, NPY, galanin, and opioids) and negative (e.g., leptin, melanocortins, corticotropin-releasing factor, glucagon-like peptide-1, and cholecystokinin) regulators of energy balance both within and outside the central nervous system (Arase et al., 1988; Rosenbaum et al., 1997).

A decline of blood glucose levels can signal the initiation of food intake (Oomura, 1980). The lateral hypothalamic area contains glucose-sensitive neurons that are

activated by glucopenia and thus implicated in the positive short-term regulation of feeding and energy expenditure (Oomura et al., 1974). It is tempting to speculate that all or some of the orexin-containing neurons may be glucose-sensitive, or that they may receive stimulatory projections from glucose-sensitive neurons. Future experiments will also determine whether orexins have additional actions relevant to nutritional homeostasis, such as effects on the regulation of systemic energy expenditure, secretion of metabolic hormones such as insulin, and ultimately, the regulation of body weight.

The present discovery of orexins and their receptors may provide a novel molecular basis for the role of the lateral hypothalamic areas in the regulation of feeding behavior. It is clear, however, that the definitive assignment of physiological roles for orexins requires further pharmacological as well as molecular genetic investigations. Nevertheless, pharmacological intervention directed at the orexin receptors may prove to be an attractive avenue toward the discovery of novel therapeutics for diseases involving disregulation of energy homeostasis, such as obesity and diabetes mellitus.

Experimental Procedures

Transfected Cells

Full-length cDNAs encoding individual orphan GPCRs were subcloned into the pCDN mammalian expression vector. These plasmids were individually transfected into the human embryonic kidney (HEK) 293 cells, and stable transfectant cell lines established and maintained as described (Aiyar et al., 1994). For in vitro pharmacological assessments (Figure 3), CHO-K1 cells were stably transfected with human *OX_1R* and *OX_2R* expression vectors, and transfected cell lines were maintained as previously described (Xu et al., 1994).

Purification of Orexin

Approximately 200 g of frozen rat whole brain (150 pieces, Pel-Freeze) were homogenized by Polytron in 10 × volume of 70% (v/v) acetone, 1 M acetic acid, and 20 mM HCl. The homogenate was centrifuged at 20,000 × g for 30 min at 4°C. The resultant supernatant was collected and extracted three times with diethyl ether. The aqueous phase was centrifuged at 20,000 × g for 30 min at 4°C, and the supernatant was loaded onto two 10 g cartridges of Sep-Pak C18 (Waters), which were preequilibrated with 0.1% (v/v) TFA. Cartridges were washed with 5% CH_3CN/0.1% TFA, and then eluted with 50% CH_3CN/0.1% TFA. The eluate was lyophilized, redissolved in 1 M acetic acid with sonication, and then filtered through a 20 μm Mirex GV filter (Millipore). Step 1 (Figure 1A): the extract was directly loaded onto a C_{18} reverse-phase HPLC column (Vydac 218TP510; 10 mm × 250 mm), preequilibrated with 3% CH_3CN/0.1% TFA at a flow rate of 3 ml/min at room temperature. A 10%–40% gradient of CH_3CN in 0.1% TFA was then applied over 100 min. Three-milliliter fractions were collected, and ≈2% of each fraction was set aside and assayed for $[Ca^{2+}]_i$ transients in OX_1R–expressing HEK293 cells (see below). Step 2 (Figure 1B): the active fractions were pooled and directly applied to a cation-exchange HPLC column (TosoHaas SP-5PW; 7.5 mm × 75 mm) preequilibrated with 20 mM Na-phosphate (pH 3.0)/30% CH_3CN at room temperature. A 0–0.5 M gradient of NaCl in 20 mM Na-phosphate (pH 3.0)/30% CH_3CN was applied over 60 min at a flow rate of 1 ml/min. One-milliliter fractions were collected, and ~3% from each fraction was used for the $[Ca^{2+}]_i$ assay. Step 3 (Figure 1C): the active fractions were pooled, diluted 4-fold with 0.1% TFA, and directly loaded onto an analytical C_{18} reverse-phase column (Vydac 218TP54; 4.6 mm × 250 mm) preequilibrated with 3% CH_3CN/0.1% TFA at a flow rate of 1 ml/min at room temperature. A 21%–36% gradient of CH_3CN in 0.1% TFA was applied over 75 min. Individual UV absorption peaks (210 nm) were collected manually, and ~3% from each fraction was assayed. Step 4 (Figure 1D): the active peak was diluted 4-fold with 0.1% TFA and directly loaded onto the same C_{18} column, but this time preequilibrated at 40°C with 3% CH_3CN/0.1% TFA. A 21%-36% gradient of CH_3CN in 0.1% TFA was applied over 75 min at 40°C. The major 210 nm peak, representing virtually pure orexin-A, was collected manually. For purification of rat orexin-B and orexin-B[3–28] as well as bovine orexin-A, basically the same procedures were used, except that step 3 was replaced with a reverse-phase HPLC under neutral pH: active fractions from step 2 were directly loaded onto the same analytical C_{18} column preequilibrated with 3% CH_3CN/20 mM Tris-HCl (pH 7.0 at 40°C). A 3%–40% gradient of CH_3CN in 20 mM Tris-HCl (pH 7.0) was applied over 74 min at 40°C. Individual 210 nm peaks were collected manually, and the active fraction was subjected to step 4 as described above.

Peptide Microsequencing

Direct sequencing of the intact orexin-A peptide by Edman degradation failed, suggesting a blocked amino terminus. The monoisotopic molecular mass of the intact peptide was determined to be 3558.7 ± 0.1 Da by time lag–focusing matrix-assisted laser desorption/ionization (MALDI) mass spectrometry (Carr and Annan, 1996) using internal peptide standards (Micromass TofSpec-SE). The measured mass of the peptide increased by 232 Da upon reaction with iodoacetamide in the presence of DTT, indicating the presence of two intramolecular disulfides bonds. Digestion of the reduced and alkylated peptide with Lys-C provided two peptides with average M_r = 1287 and 2530. Edman sequence of the mixture provided a single partial sequence of TCSCRLYELLHGAGNHAAG. Edman sequence analysis of an Asn-C digest mixture extended the C-terminal sequence as follows . . . HAAGILTL. The C-terminal sequence, . . . EXX HGAGNHAAGXXTX (where X is either Leu or Ile), was also confirmed by MALDI mass spectrometry of the peptide partially digested with carboxypeptidase Y (Voyager Elite XL, PerSeptive Biosystems). The blocked N-terminal Lys-C peptide was sequenced by nanoelectrospray collision induced dissociation (CID) tandem mass spectrometry (Carr et al., 1996; Wilm and Mann, 1996) on a triple quadrupole mass spectrometer (Perkin-Elmer Sciex API-III). A sequence of <EPXPDCCRQK (calculated MH^+ = 1286.6) was determined from the tandem MS data, where <E is pyroglutamic acid, and X is either Leu or Ile. The identity and sequence of the first two residues were confirmed by MS^3 of the b2 ion produced by in-source CID. X was determined to be Leu by amino acid analysis of the HPLC purified N-terminal peptide. The Gln residue at position 9 was distinguished from Lys (both amino acids have the same residue mass) by acetylation of the peptide and remeasurement of the molecular weight. The MH^+ ion for the ligand shifted by 42 Da from 1286.6 to 1328.6, indicating the addition of only one acetate group (calculated MH^+ = 1328.6). Because Gln residues cannot be acetylated and the N terminus is blocked, the addition of only one acetate group strongly suggests the C-terminal sequence is QK, not KK. The M_r determined for the intact peptide (3558.7 ± 0.1 Da) indicates that the C terminus is an amide rather than a free acid and that all four Cys are in disulfide linkages (calculated monoisotopic M_r = 3558.7).

Cloning of Rat *prepro-orexin* cDNA

A part of the orexin-A sequence, QPLPDCCRQKTCSCRLYELLHGA GNHAAGI (amino acids 1–30), was chosen to design highly degenerate oligonucleotide primers encoding its ends: 5′-CA(A,G)CCN(C,T)T NCCNGA(C,T)TG(C,T)TG-3′ and 5′-ATNCCNGCNGC(A,G)TG(A,G)TT-3′. A cDNA fragment correctly encoding the peptide was obtained by RT–PCR using rat brain poly(A) RNA as template. A nondegenerate oligonucleotide primer, 5′-GTTGCCAGCTCCGTGCAACAGTTCGTA GAGACGG-3′, was designed based on the sequence of the RT–PCR product. Double-stranded cDNA was synthesized from rat brain poly(A) RNA, ligated to the Marathon adaptor (Clontech), and used as template for the initial 5′-RACE reaction with Adaptor Primer 1 (Clontech) and the above specific primer. A nested PCR reaction was performed using an oligonucleotide, 5′-CGGCAGGAACACGTC TTCTGGCG-3′, and the Adaptor Primer 2 (Clontech). An approximately 250 bp 5′ cDNA product, correctly encoding the peptide, was obtained. Single-stranded rat brain cDNA was then synthesized using an oligonucleotide, 5′-CCTCTGAAGGTTCCAGAATCGATAG $(T)_{25}$(A,C,G)N-3′, as a specific primer for the reverse transcription.

This was used as template for a 3′-RACE reaction using a specific primer, 5′-TCCTTGGGTATTTGGACCACTGCACCGAAG-3′ (corresponding to a part of the 5′-noncoding region of the cDNA sequence obtained by the 5′-RACE), and an anchor primer, 5′-CCTCTGAAGGT TCCAGAATCGATAG-3′. The product was subjected to a nested PCR reaction using an oligonucleotide, 5′-ATACCATCTCTCCGGAT TGCCTCTCCCTGA-3′, and the same anchor primer. A discrete 0.6 kb product containing the correct 5′ cDNA sequence was obtained. The full-length cDNA sequence was determined by resequencing the products obtained from three independent 3′-RACE reactions.

Cloning of Human and Mouse *prepro-orexin* Genes

Since we found that the full-length rat *prepro-orexin* cDNA, which contains CTG triplet repeats (encoding the oligo-leucine stretch in the signal sequence), tends to cross-hybridize with a number of unrelated genes, we produced a cDNA probe that did not contain the repeats by RT–PCR from rat brain RNA, using primers 5′-CAGCC TCTGCCCGACTGCTGT-3′ and 5′-CGTCTTTATTGCCTAGGGACTG GCGAGGAG-3′. Human and mouse genomic libraries (Clontech and Stratagene, respectively) were screened by plaque hybridization to this cDNA probe. Resulting genomic fragments containing the entire *prepro-orexin* coding sequences were further characterized and sequenced by standard procedures.

Cloning of *OX_1R* and *OX_2R* cDNAs

Cloning of full-length human *OX_1R* (HFGAN72) cDNA has been disclosed elsewhere (US Patent No. WO96/34877; November 7, 1996) (Figure 2C). Rat *OX_1R* cDNA was obtained by screening rat brain cDNA libraries with the full-length human *OX_1R* cDNA as probe, using standard procedures. In order to clone full-length human *OX_2R* cDNA, an inter-EST RT–PCR was performed with human brain poly(A)$^+$ RNA as template, using oligonucleotide primers based on the public 5′ and 3′ EST sequences (GenBank accession numbers D81887 and W86548, respectively). The resultant cDNA product, which contained a large part of the coding region spanning the transmembrane domains 1–7, was further extended by standard 5′-RACE and 3′-RACE procedures. Rat *OX_2R* cDNA was obtained by screening rat brain cDNA libraries with the full-length human *OX_2R* cDNA as probe.

Radiation Hybrid Mapping

The following oligonucleotides were used to amplify genomic fragments: *prepro-orexin*, GCCAAAGGTGTCTCCACTC and GACAGGT GCAAACGGAGCAC; *OX_1R*, GGTGCTCACCAGCGTCACCAC and GCTTAATCCTCACATCAACCCTGC; *OX_2R*, GAGGAGCTTGCAGCAT TGAGC and GTGCAGGTATTCCCTCCACAG. PCR of the *prepro-orexin*, *OX_1R*, and *OX_2R* genes was performed in duplicates against the 96 samples (including 3 controls: donor DNA, host DNA, and water) in the GeneBridge 4 radiation hybrid panel (Research Genetics) (Gyapay et al., 1996). The scoring strings of 93 × 1's (presence), 0's (absence), and 2's (ambiguous) were submitted to the Radiation Hybrid Mapping Server at MIT (http://www.genome.wi.mit.edu/) (Hudson et al., 1995). Cytogenetic locations were inferred from these results using the markers shown to neighbor the genes via The Genome Directory (1995), and GDB (http://gdbwww.gdb.org/gdb/docs/gdbhome.html). Chromosomal locations were confirmed by PCR on the BIOS panel (BIOS, USA) using the same oligo pairs and conditions.

Radioligand Binding Assay

Synthetic human orexin-A was ^{125}I-labeled at Tyr17 by Chloramine-T oxidation in the presence of Na^{125}I (2,000 Ci/mmol, New England Nuclear), and monoiodinated peptide was purified by C^{18} reverse-phase HPLC as described (Takigawa et al., 1995). Stable transfectant CHO cell lines expressing human *OX_1R* or *OX_2R* were each seeded onto 12-well plates at a density of 3×10^5 cells per well. After an overnight culture, medium was discarded and cells were incubated at 20°C for 90 min with binding buffer (HEPES-buffered saline/0.5% bovine serum albumin) containing 10^{-10} M [^{125}I]orexin-A plus designated concentrations of unlabeled competitors. Cells were then washed three times with ice-cold phosphate-buffered saline, lysed in 0.1 N NaOH, and cell-bound radioactivity was determined by a γ-counter.

Intracellular Calcium Transient Assay

Stable transfectant HEK293 cells expressing orphan GPCRs were loaded with Fura-2 AM in suspension, and $[Ca^{2+}]_i$ transients evoked by agonists were monitored by a Model CAF-110 Intracellular Ion Analyser (JASCO) in 500 μl cuvette as previously described (Grynkiewicz et al., 1985; Xu et al., 1994). For in vitro pharmacological characterization (Figure 3), the same procedures were performed using stably transfected CHO cells expressing human *OX_1R* or *OX_2R*.

In Situ Hybridization

A 0.29 kb segment of rat cDNA encoding Gln33-Ser128 of prepro-orexin was generated as described above and subcloned into pBluescript II SK(+) vector. Sense and anti-sense riboprobes were generated with T7 and T3 RNA polymerases, respectively, using the Maxiscript kit (Ambion) in the presence of ^{35}S-CTP (Amersham). In situ hybridization to adult rat brain sections was performed as described (Benjamin et al., 1997).

Immunohistochemistry

Anti-orexin-A antiserum was raised in rabbits by immunization with synthetic orexin-A[14–33], CRLYELLHGAGNHAAGILTL-amide, conjugated to keyhole limpet hemocyanin (Calbiochem) using 3-maleimidobensoic acid N-hydroxysuccimide ester (Sigma). Antiserum was affinity purified on an orexin-A-conjugated Sepharose CL-4B (Pharmacia) column and used for immunohistochemistry. Male Sprague-Dawley rats (~300 g) were anesthetized and perfused via the left cardiac ventricle with phosphate-buffered saline (PBS). Brain was taken out, directly embedded in OCT compound (Tissue-Tek), and frozen in liquid nitrogen. Cryostat sections (15 μm) were cut and mounted on silane-coated glass sides. The sections were post-fixed with 4% paraformaldehyde in 0.1 M phosphate buffer (pH 7.2) for 1 hr and washed three times in PBS. The sections were incubated with 1% bovine serum albumin in PBS for 1 hr and then incubated with affinity-purified antiserum in the same solution for 1 hr at room temperature. After washing three times in PBS, the sections were incubated with FITC-conjugated goat anti-rabbit IgG antibody (Cappel) for 1 hr at room temperature. Slides were then washed three times in PBS and examined under fluorescence microscope.

Intracerebroventricular Administration of Orexins

Male Wistar rats (180–200 g on arrival; Charles-River) were housed under controlled lighting (12 hr light-dark cycle) and temperature (22°C) conditions. Food (standard chow pellets) and water were available ad libitum. Rats (200–220 g) were anesthetized with pentobarbital (50 mg/kg i.p.), positioned in a Koph Model 900 stereotaxic frame, and implanted with a guide cannula into the left lateral ventricle under sterile conditions using a MEDIBIO Optical Brain Tracer (Muromachi Kikai) (Ikeda and Matsushita, 1980). The coordinates used to map the correct positioning of the implants were: 6.1 mm anterior to the lambda, 1.5 mm lateral from the midline, and ~3.4 mm (guided by MEDIBIO) ventral to the skull surface, with the incisor bar set 3.3 mm below the interauricular line. Rats were then housed singly under the same conditions as above for a recovery period of at least 7 days, and body weights were monitored daily for the duration of the study. After recovery from surgery, rats were transferred to grid-floor cages and fed with powdered chow so that food intake measurements could be made. The rats were acclimated to the new environment at least for 1 day. The position of the cannula was verified by central administration of human NPY (3 nmol in sterile water); for a positive test, at least 8 g of food was eaten over a 4 hr period postinjection. Only positively testing animals ($n = 8$–10) were used. The studies were conducted according to a multidose, crossover design, with the order of dosing determined using the Latin square principle, leaving at least one rest day between administrations. All doses were delivered in a volume of 5 μl in sterile water over 30 s, and the injector remained in position for a further 30 s to ensure complete dispersal of the peptide. All intracerebroventricular administrations began at 2 h into light cycle, and food

intake was measured at 1, 2, and 4 h intervals. All peptides were dissolved in sterile water, initially at 6 mM, and diluted in water as needed. Water alone was used for the vehicle control.

Acknowledgments

We thank Katsutoshi Goto for discussion, Tadahiro Nambu for technical assistance in immunohistochemistry, and Mike Brown and Joe Goldstein for critically reading the manuscript. We also thank the following scientists at SmithKline Beecham for their various contributions: Neil Upton, Christine Debouck, Catherine Ellis, Ganesh Sathe, Michael Huddleston, Jeff Stadel, John Martin, Lily Zhang, Paul Lysko, and Mary Brawner. M. Y. is an Investigator and T. S. and A. A. are Associates of the Howard Hughes Medical Institute. R. M. C. is an NIH fellow of the Pediatric Scientist Development Program. M. I. is a Summer Undergraduate Research Fellow of the University of Texas Southwestern Medical Center. This work was supported in part by research grants from the Perot Family Foundation.

Received December 12, 1997; revised January 7, 1998.

References

Aiyar, N., Baker, E., Wu, H.-L., Nambi, P., Edwards, R.M., Trill, J.J., Ellis, C., and Bergsma, D.J. (1994). Human AT_1 receptor is a single copy gene: characterization in a stable cell line. Mol. Cell Biochem. *131*, 75–86.

Arase, K., York, D.A., Shimizu, H., Shargill, N., and Bray, G.A. (1988). Effects of corticotropin-releasing factor on food intake and brown adipose tissue thermogenesis in rats. Am. J. Physiol. *255*, E255–259.

Bateman, A., Solomon, S., and Bennett, H.P.J. (1990). Post-translational modification of bovine pro-opiomelanocortin. J. Biol. Chem. *265*, 22130–22136.

Benjamin, I.J., Shelton, J., Garry, D.J., and Richardson, J.A. (1997). Temporospatial expression of the small HSP/αB-crystallin in cardiac and skeletal muscle during mouse development. Dev. Dyn. *208*, 75–84.

Bernardis, L.L., and Bellinger, L.L. (1993). The lateral hypothalamic area revisited: neuroanatomy, body weight regulation, neuroendocrinology and metabolism. Neurosci. Biobehav. Rev. *17*, 141–193.

Bernardis, L.L., and Bellinger, L.L. (1996). The lateral hypothalamic area revisited: ingestive behavior. Neurosci. Biobehav. Rev. *20*, 189–287.

Bing, C., Wang, Q., Pickavance, L., and Williams, G. (1996). The central regulation of energy homoeostasis: roles of neuropeptide Y and other brain peptides. Biochem. Soc. Trans. *24*, 559–565.

Bittencourt, J.C., Presse, F., Arias, C., Peto, C., Vaughan, J., Nahon, J.-L., Vale, W., and Sawchenko, P.E. (1992). The melanin-concentrating hormone system of the rat brain: an immuno- and hybridization histochemical characterization. J. Comp. Neurol. *319*, 218–245.

Bradbury, A.F., and Smyth, D.G. (1991). Peptide amidation. Trends Biochem. Sci. *16*, 112–115.

Bray, G.A. (1995). Obesity, fat intake, and chronic disease. In Psychopharmacology: The Fourth Generation of Progress, F.E. Bloom and D.J. Kupher, eds. (New York: Raven Press), pp. 1591–1608.

Busby, W.H., Jr., Quackenbush, G.E., Humm, J., Youngblood, W.W., and Kizer, J.S. (1987). An enzyme(s) that converts glutaminyl-peptides into pyroglutamyl-peptides. J. Biol. Chem. *262*, 8532–8536.

Carr, S.A., and Annan, R.S. (1996). Overview of peptide and protein analysis by mass spectrometry. In Current Protocols in Protein Science (New York: John Wiley and Sons, Inc.).

Carr, S.A., Huddleston, M.J., and Annan, R.S. (1996). Selective detection and sequencing of phosphopeptides at the femtomole level by mass spectrometry. Anal. Biochem. *239*, 180–192.

Chen, H., Charlat, O., Tartaglia, L.A., Woolf, E.A., Weng, X., Ellis, S.J., Lakey, N.D., Culpepper, J., Moore, K.J., Breitbart, R.E., et al. (1996). Evidence that the diabetes gene encodes the leptin receptor: identification of a mutation in the leptin receptor gene in *db*/*db* mice. Cell *84*, 491–495.

Eipper, B.A., Milgram, S.L., Husten, E.J., Yun, H.Y., and Mains, R.E. (1993). Peptidylglycine alpha-amidating monooxygenase: a multifunctional protein with catalytic, processing, and routing domains. Protein Sci. *2*, 489–497.

Erickson, J.C., Clegg, K.E., and Palmiter, R.D. (1996a). Sensitivity to leptin and susceptibility to seizures of mice lacking neuropeptide Y. Nature *381*, 415–418.

Erickson, J.C., Hollopeter, G., and Palmiter, R.D. (1996b). Attenuation of the obesity syndrome of *ob/ob* mice by the loss of neuropeptide Y. Science *274*, 1704–1707.

Fan, W., Boston, B.A., Kesterson, R.A., Hruby, V.J., and Cone, R.D. (1997). Role of melanocortinergic neurons in feeding and the *agouti* obesity syndrome. Nature *385*, 165–168.

Friedman, J.M. (1997). The alphabet of weight control. Nature *385*, 119–120.

Gerald, C., Walker, M.W., Criscione, L., Gustafson, E.L., Batzl-Hartmann, C., Smith, K.E., Vaysse, P., Durkin, M.M., Laz, T.M., Linemeyer, D.L., et al. (1996). A receptor subtype involved in neuropeptide-Y-induced food intake. Nature *382*, 168–171.

Grynkiewicz, G., Poenie, M., and Tsien, R.Y. (1985). A new generation of Ca^{2+} indicators with greatly improved fluorescence properties. J. Biol. Chem. *260*, 3440–3450.

Gyapay, G., Schmitt, K., Fizames, C., Jones, H., Vega-Czarny, N., Spillet, D., Muselet, D., Prud'Homme, J.F., Dib, C., Auffray, C., et al. (1996). A radiation hybrid map of the human genome. Hum. Mol. Genet. *5*, 339–346.

Hardman, J.G., Gilman, A.G., and Limbird, L.E. (1996). The Pharmacological Basis of Therapeutics, 9th Ed. (New York: McGraw-Hill).

Hepler, J.R., Kozasa, T., and Gilman, A.G. (1994). Purification of recombinant Gq alpha, G11 alpha, and G16 alpha from Sf9 cells. Meth. Enzymol. *237*, 191–212.

Hudson, T., Stein, L., Gerety, S., Ma, J., Castle, A., Silva, J., Slonim, D., Baptista, R., Kruglyak, L., Xu, S., et al. (1995). An STS-based map of the human genome. Science *270*, 1945–1954.

Huszar, D., Lynch, C.A., Fairchild-Huntress, V., Dunmore, J.H., Fang, Q., Berkemeier, L.R., Gu, W., Kesterson, R.A., Boston, B.A., Cone, R.D., et al. (1997). Targeted disruption of the melanocortin-4 receptor results in obesity in mice. Cell *88*, 131–141.

Ikeda, M., and Matsushita, A. (1980). Reflectance of rat brain structures mapped by an optical fiber technique. J. Neurosci. Meth. *2*, 9–17.

Jacobowitz, D.M., and O'Donohue, T.L. (1978). α-melanocyte stimulating hormone: immunohistochemical identification and mapping in neurons of rat brain. Proc. Natl. Acad. Sci. USA *75*, 6300–6304.

Mountjoy, K.G., Mortrud, M.T., Low, M.J., Simerly, R.B., and Cone, R.D. (1994). Localization of the melanocortin-4 receptor (MC4-R) in neuroendocrine and autonomic control circuits in the brain. Mol. Endocrinol. *8*, 1298–1308.

Munson, P.J., and Rodbard, D. (1980). LIGAND: A versatile computerized approach for characterization of ligand-binding systems. Anal. Biochem. *107*, 220–239.

Ohki-Hamazaki, H., Watase, K., Yamamoto, K., Orura, H., Yamano, M., Yamada, K., Maeno, H., Imaki, J., Kikuyama, S., Wada, E., and Wada, K. (1997). Mice lacking bombesin receptor subtype-3 develop metabolic defects and obesity. Nature *390*, 165–169.

Ollmann, M.M., Wilson, B.D., Yang, Y.-K., Kerns, J.A., Chen, Y., Gantz, I., and Barsh, G.S. (1997). Antagonism of central melanocortin receptors in vitro and in vivo by Agouti-related protein. Science *278*, 135–138.

Oomura, Y. (1980). Input-output organization in the hypothalamus relating to food intake behavior. In Handbook of the Hypothalamus, Volume 2: Physiology of the Hypothalamus, P.J. Morgane and J. Panksepp, eds. (New York: Marcel Dekker), pp. 557-620.

Oomura, Y., Ooyama, H., Sugimori, M., Nakamura, T., and Yamada, Y. (1974). Glucose inhibition of the glucose-sensitive neurone in the rat lateral hypothalamus. Nature *247*, 284–286.

Paxinos, G., and Watson, C. (1986). The Rat Brain in Stereotaxic Coordinates (San Diego: Academic Press).

Qu, D., Ludwig, D.S., Gammeltoft, S., Piper, M., Pelleymounter, M.A.,

Cullen, M.J., Mathes, W.F., Przypek, J., Kanarek, R., and Maratos-Flier, E. (1996). A role for melanin-concentrating hormone in the central regulation of feeding behaviour. Nature *380*, 243–247.

Rosenbaum, M., Leibel, R.L., and Hirsch, J. (1997). Obesity. N. Engl. J. Med. *337*, 396–407.

Rouille, Y., Dugay, S.J., Lund, K., Furuta, M., Gong, Q., Lipkind, G., Oliva, A.A., Jr., Chan, S.J., and Steiner, D.F. (1995). Proteolytic processing mechanisms in the biosynthesis of neuroendocrine peptides: the subtilisin-like proprotein convertases. Front. Neuroendocrinol. *16*, 322–361.

Shughrue, P.J., Lane, M.V., and Merchenthaler, I. (1996). Glucagon-like peptide-1 receptor (GLP1-R) mRNA in the rat hypothalamus. Endocrinology *137*, 5159–5162.

Shutter, J.R., Graham, M., Kinsey, A.C., Scully, S., Lüthy, R., and Stark, K.L. (1997). Hypothalamic expression of ART, a novel gene related to *agouti*, is up-regulated in *obese* and *diabetic* mutant mice. Genes Dev. *11*, 593–602.

Stadel, J.M., Wilson, S., and Bergsma, D. (1997). Orphan G protein–coupled receptors: a neglected opportunity for pioneer drug discovery. Trends Pharmacol. Sci. *18*, 430–437.

Stephens, T.W., Basinski, M., Bristow, P.K., Bue-Valleskey, J.M., Burgett, S.G., Craft, L., Hale, J., Hoffmann, J., Hsiung, H.M., Kriauciunas, A., et al. (1995). The role of neuropeptide Y in the antiobesity action of the *obese* gene product. Nature *377*, 530–532.

Takigawa, M., Sakurai, T., Kasuya, Y., Abe, Y., Masaski, T., and Goto, K. (1995). Molecular identification of guanine-nucleotide-binding regulatory proteins which couple to endothelin receptors. Eur. J. Biochem. *228*, 102–108.

Tartaglia, L.A., Dembski, M., Weng, X., Deng, N., Culpepper, J., Devos, R., Richards, G.J., Campfield, L.A., Clark, F.T., Deeds, J., et al. (1995). Identification and expression cloning of a leptin receptor, OB-R. Cell *83*, 1263–1271.

Turton, M.D., O'Shea, D., Gunn, I., Beak, S.A., Edwards, C.M.B., Meeran, K., Choi, S.J., Taylor, G.M., Heath, M.M., Lambert, P.D., et al. (1996). A role for glucagon-like peptide-1 in the central regulation of feeding. Nature *379*, 69–72.

von Heijne, G. (1986). A new method for predicting signal sequence cleavage sites. Nucleic Acids Res. *14*, 4683–4690.

Warembourg, M., and Jolivet, A. (1993). Immunocytochemical localization of progesterone receptors in galanin neurons in the guinea pig hypothalamus. J. Neuroendocrinol. *5*, 487–491.

Wijker, M., Wszolek, Z.K., Wolters, E.C.H., Rooimans, M.A., Pals, G., Pfeiffer, R.F., Lynch, T., Rodnitzky, R.L., Wilhelmsen, K.C., and Arwert, F. (1996). Localization of the gene for rapidly progressive autosomal dominant parkinsonism and dementia with pallido-ponto-nigral degeneration to chromosome 17q21. Hum. Mol. Genet. *5*, 151–154.

Wilhelmsen, K.C. (1997). Frontotemporal dementia is on the MAPtau. Ann. Neurol. *41*, 139–140.

Wilhelmsen, K.C., Lynch, T., Pavlou, E., Higgins, M., and Hygaard, T.G. (1994). Localization of disinhibition-dementia-parkinsonism-amyotrophy complex to 17q21–22. Am. J. Hum. Genet. *55*, 1159–1165.

Wilm, M., and Mann, M. (1996). Analytical properties of the nanoelectrospray ion source. Anal. Chem. *68*, 1–8.

Wolf, G. (1997). Neuropeptides responding to leptin. Nutr. Rev. *55*, 85–88.

Xu, D., Emoto, N., Giaid, A., Slaughter, C.A., Kaw, S., de Wit, D., and Yanagisawa, M. (1994). ECE-1: A membrane-bound metalloprotease that catalyzes the proteolytic activation of big endothelin-1. Cell *78*, 473–485.

Yen, T.T., Gill, A.M., Frigeri, L.G., Barsh, G.S., and Wolff, G.L. (1994). Obesity, diabetes, and neoplasia in yellow $A^{vy}/-$ mice: ectopic expression of the *agouti* gene. FASEB J. *8*, 479–488.

Zarjevski, N., Cusin, I., Vettor, R., Rohner-Jeanrenaud, F., and Jeanrenaud, B. (1993). Chronic intracerebroventricular neuropeptide-Y administration to normal rats mimics hormonal and metabolic changes of obesity. Endocrinology *133*, 1753–1758.

Zhang, Y., Proenca, R., Maffei, M., Barone, M., Leopold, L., and Friedman, J.M. (1994). Positional cloning of the mouse *obese* gene and its human homologue. Nature *372*, 425–432.

GenBank Accession Numbers

The following full-length nucleotide sequences have been submitted to GenBank (accession number in parentheses): *prepro-orexin* cDNAs, human (AF041240), rat (AF041241), and mouse (AF041242); OX_1R cDNAs, human (AF041243) and rat (AF041244); and OX_2R cDNAs, human (AF041245) and rat (AF041246).